Supporting Information

Fucosylated molecules competitively interfere with cholera toxin binding to host cells

Amberlyn M. Wands[1], Jakob Cervin[2], He Huang[3], Ye Zhang[3], Gyusaang Youn[3], Chad A. Brautigam[4], Maria Matson Dzebo[5], Per Björklund[6], Ville Wallenius[6], Danielle K. Bright[7], Clay S. Bennett[7], Pernilla Wittung-Stafshede[5], Nicole S. Sampson[3], Ulf Yrlid[2], Jennifer J. Kohler[1]*

[1]Department of Biochemistry, 5323 Harry Hines Blvd., UT Southwestern Medical Center, Dallas, TX 75390-9038, United States; [2]Department of Microbiology and Immunology, Institute of Biomedicine, University of Gothenburg, SE-40530 Gothenburg, Sweden; [3]Department of Chemistry, 100 Toll Rd., Stony Brook University, Stony Brook, NY 11790-3400, United States; [4]Departments of Biophysics and Microbiology, 5323 Harry Hines Blvd., UT Southwestern Medical Center, Dallas, TX 75390-8816, United States; [5]Chalmers University of Technology, Department of Biology and Biological Engineering, SE-41296 Gothenburg, Sweden; [6]Department of Gastrosurgical Research and Education, Sahlgrenska Academy, University of Gothenburg, Sahlgrenska University Hospital/Östra, Gothenburg, Sweden; [7]Department of Chemistry, 62 Talbot Ave, Tufts University, Medford, MA 02155, United States

Contents:

Colitose Synthesis

Scheme S1.

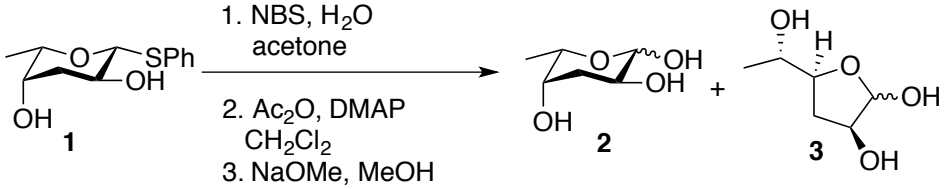

Colitose preparation: A solution of known colitose derivative **1**[1] (0.44 g, 1.83 mmol) in acetone (30.0 mL) and water (2.0 mL) was cooled to 0 °C and treated with *N*-bromosuccinimide (0.27 g, 1.52 mmol). After 50 min, the reaction was concentrated, and the residue was suspended in 16.0 mL CH_2Cl_2. The reaction mixture was treated with triethylamine (2.7 mL, 19.4 mmol) and 4-(dimethylamino)pyridine (0.06 g, 0.4 mmol). The suspension was stirred for 10 min, then treated with acetic anhydride (1.45 mL, 15.3 mmol). The resulting solution was stirred at room temperature for 75 min, and then concentrated *in vacuo*. The residue was dissolved in 4 mL MeOH and treated with NaOMe (0.01g, 0.2 mmol). After 160 min the reaction was treated with a freshly prepared solution of NaOMe in MeOH (0.1 M, 4.7 ml, 0.5 mmol) and stirring continued. Once the reaction was complete by TLC the reaction was quenched by the addition of amberlite IR-120 resin, filtered, and concentrated *in vacuo*. Flash column chromatography (SiO_2, 15% MeOH in CH_2Cl_2) afforded the target compound (0.18 g, 1.2 mmol 66%) as a mixture of α/β pyranoses (**2**) and α/β furanoses (**3**), in accordance with the literature.[2] ^{1}H-NMR showed good agreement with the literature.[2]

^{1}H-NMR (500 MHz, CD_3OD): d 5.06 (s, 0.4H), 5.09 (d, *J* = 9.2 Hz, 0.1 H), 5.02 (d, *J* = 3.3 Hz, 0.4 Hz), 4.59 (s, 0.1 Hz); 4.38 (d, *J* = 7.7 Hz), 4.27-4.20 (m, 0.1 H), 4.15-4.05 (m, 1H), 4.02-4.-1 (m, 0.4 Hz); 3.96-3.92 (m, 0.4 H)3.73-3.64 (m, 3H), 3.61-3.56 (m, 1H), 2.39-2.34 (m, 0.4 H), 2.24-2.17 (m, 0.1 H), 2.16-2.11 (m, 1H), 1.96 (dt, *J* = 9.4, 2.9 Hz, 0.4 H), 1.88 (ddd, *J* = 12.7, 3.9, 3.9 Hz, 0.4 Hz), 1.74-1.68 (m, 0.1 H), 1.65-1.47 (m, 1.4 H), 1.20-1.11 (m, 5.7 H).

^{13}C-NMR (125 MHz, CD_3OD): d 102.2, 98.2, 95.2, 91.6, 82.2, 81.2, 75.4, 74.2, 71.1, 70.9, 69.6, 68.4, 68.3, 66.4, 66.1, 63.1, 37.1, 33.8, 32.2, 31.6, 18.3, 17.9, 15.8, 15.6.

Polymer Synthesis

Materials: Unless otherwise noted, all reagents were used as supplied by commercial suppliers without further purification. $(H_2IMes)(3\text{-}BrPyr)_2Cl_2Ru{=}CHPh$ was prepared according to the literature.[3] CH_2Cl_2, benzene, Et_2O, THF and CH_3OH were dried in a GlassContour solvent pushstill system.

Methods: All reactions were carried out under an Ar or N_2 atmosphere in oven-dried glassware unless otherwise specified. Analytical thin layer chromatography (TLC) was performed with precoated silica gel plates (60F254), flash chromatography was performed with silica gel-60 (230–400 mesh) and Combi-Flash chromatography with RediSep normal phase silica columns (Teledyne Isco, silica gel-60, 230–400 mesh). Bruker 400 and Bruker 500 MHz NMR instruments were used to perform NMR analyses. ^{1}H-NMR spectra are reported as chemical shift in parts per million (multiplicity, coupling constant in Hz, integration) and were acquired in $CDCl_3$ unless otherwise noted. ^{1}H-NMR data are assumed to be first order.

For $Đ_m$ (dispersity index) determination, polymers (before flash column chromatography purification) were dissolved in THF (0.5 mg/mL). An aliquot (100 µL) of the polymer solution was injected and analyzed by gel permeation chromatography using a Phenogel column (300 x 7.80 mm, 5 µm, linear mixed bed, 0-500k MW range). Elution was performed at 0.7 mL/min with THF and RI detection at 30 °C. Narrowly dispersed polystyrene standards from Aldrich or Agilent were used to check static light scattering molecular weight calibration. The number average and weight average molecular weights were calculated utilizing a differential refractometer and a multi-angle light scattering detector and are based on the static light scattering signal.

Random glycopolymer preparations: The norbornene fucose, glucose monomers and $poly(NBGlc)_{100}$ were synthesized as described.[4] Fucose monomers (50 eq), glucose monomers (50 eq) and 3rd generation Grubbs catalyst $(H_2IMes)(3\text{-Br-pyr})_2Cl_2Ru{=}CHPh$ (1 eq) were mixed in CH_2Cl_2 to achieve a final monomer concentration of 57 mM and allowed to react at RT. The reaction was monitored by TLC. After all monomers were consumed, the polymerizations were quenched with excess ethyl vinyl ether. Poly-$(NBAc_3Fuc_{50}$-*ran*-$NBAc_4Glc_{50})$ was purified by precipitation in cold ether. The structures of glycopolymers were confirmed by ^{1}H NMR analysis:

$poly(NBAc_4Glc)_{100}$. Yield after purification: 75%. ^{1}H NMR (500 MHz, $CDCl_3$): δ 5.78-6.0 (m), 5.23-5.48 (with max at 5.28, 5.32), 5.20 (br s), 5.07 (br s), 4.96 (br s), 4.55 (br s), 4.28 (br s), 4.13 (br s), 3.84 (br s), 3.63-3.77 (with max at 3.70, 3.75), 3.18-3.62 (with max at 3.30, 3.50, 3.53), 3.03 (br s), 2.67 (br s), 2.20-2.37 (with max at 2.37, 2.33), 1.90-2.20 (with max at 1.94, 2.02, 2.05, 2.10, 2.19), 1.75 (br s), 1.60 (br s), 0.97-1.39 (m).

poly-$(NBAc_3Fuc_{50}$-*ran*-$NBAc_4Glc_{50})$: Yield after purification: 92%. ^{1}H NMR (400 MHz, $CDCl_3$): δ 6.09 (br s), 5.63-4.86 (m), 4.53 (br s), 4.27 (br s), 4.20-4.02 (m), 3.95-3.22 (m), 3.17-2.51(with max at 3.17, 2.92, 2.84), 2.51-1.75 (with max 2.41, 2.19, 2.14, 1.83), 1.73 (br s), 1.39-1.02 (with max at 1.26,1.11).

The number-average molecular weights (M_n), the weight average molecular weights (M_w) and dispersity index ($Đ_M$) of polymers were characterized by GPC and the results are summarized in Table S1:

Table S1. Molecular weights and dispersities of polymers.

Polymer	M_n^{theor} (kDa)	M_n^a (kDa)	M_w^a (kDa)	$Đ_M^a$
poly($NBAc_4Glc$)$_{100}$ – batch 1[b]	51.257	26.9	31.5	1.17
poly($NBAc_4Glc$)$_{100}$ – batch 2[b]	51.257	38.0	38.7	1.02
poly-($NBAc_3Fuc_{50}$-*ran*-$NBAc_4Glc_{50}$) – batch 1[b]	48.355	62.9	66.5	1.06
poly-($NBAc_3Fuc_{50}$-*ran*-$NBAc_4Glc_{50}$) – batch 2[b]	48.355	36.0	36.1	1.01

[a]Determined from GPC utilizing a differential refractometer and a multi-angle light scattering detector. Molecular weights are based on the static light scattering signal. [b]Batch 1 polymers were used for experiments with T84 and Colo205 cells; batch 2 polymers were used for experiments with primary human jejunal epithelial cells.

General procedures for deprotected glycopolymer preparation: The glycopolymers were deprotected under basic conditions and quenched with aqueous HCl following the procedure of Wu and Sampson.[4] The structures of glycopolymers were confirmed by ^{1}H NMR analysis:

poly($NBGlc$)$_{100}$: Yield after purification: 60%. ^{1}H NMR (500 MHz, D_2O): δ 5.08—5.50 (m), 4.34 (br s), 3.85 (br s), 3.66 (br s), 3.18—3.50 (with max at 3.73, 3.78, 3.80), 2.20—3.10 (with max at 2.40, 2.68, 2.98), 1.30—2.10 (with max at 1.59, 1.98), 1.09 (br s).

poly($NBFuc_{50}$-*ran*-$NBGlc_{50}$): Yield after purification: 41%. ^{1}H NMR (500 MHz, D_2O): δ 5.39 (br s), 4.47 (br s), 4.11 – 2.22 (m), 1.82 (d), 1.38 – 0.98 (m).

All reported molar polymer concentrations are based on the weight of polymer used and a theoretical M_n for polymers composed of 100 monomer units:

Table S2. Molecular weights of polymers used for concentration calculations.

Polymer	M_n^{theor} (kDa)
poly($NBGlc$)$_{100}$	34.442
poly-($NBFuc_{50}$-*ran*-$NBGlc_{50}$)	33.642

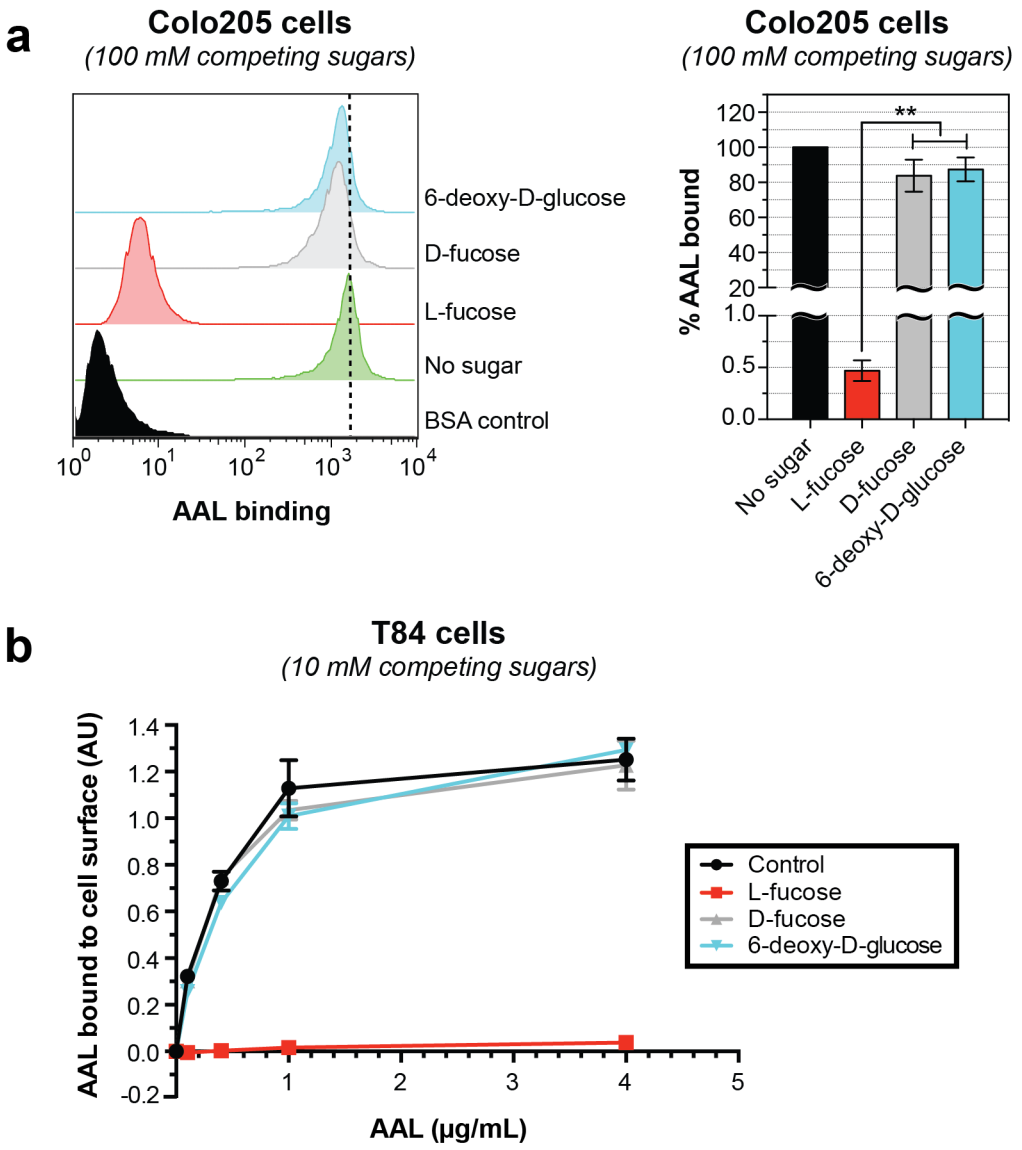

Figure S1. Blocking of AAL binding by stereochemical analogs of L-fucose. (**a**) Inhibition of AAL binding to Colo205 cells with 100 mM competing sugars in a flow cytometry assay. Histograms are representative of a single trial from three independent experiments. Bar graph shown represents the average median fluorescence intensity (MFI) from three independent experiments and their standard deviations. Statistical significance determined by unpaired Welch's test: ** indicates a *p* value < 0.01. (**b**) Inhibition of AAL binding to T84 cells with 10 mM competing sugars as measured by ELISA. Error bars represent the standard deviation from the mean (n = 2).

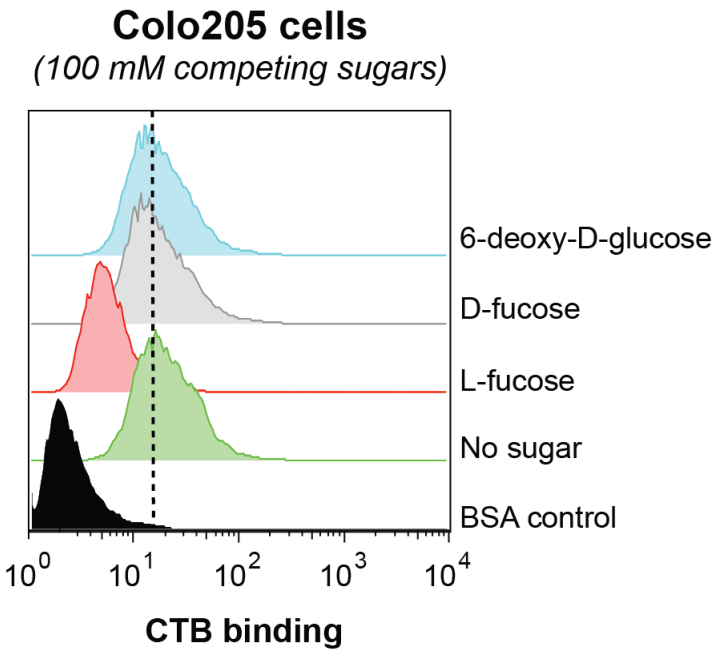

Figure S2. Flow cytometry histograms of CTB blocking by stereoisomers of L-fucose. Inhibition of CTB binding to Colo205 cells was conducted with 100 mM competing sugars. Histograms are representative of a single trial from three independent experiments.

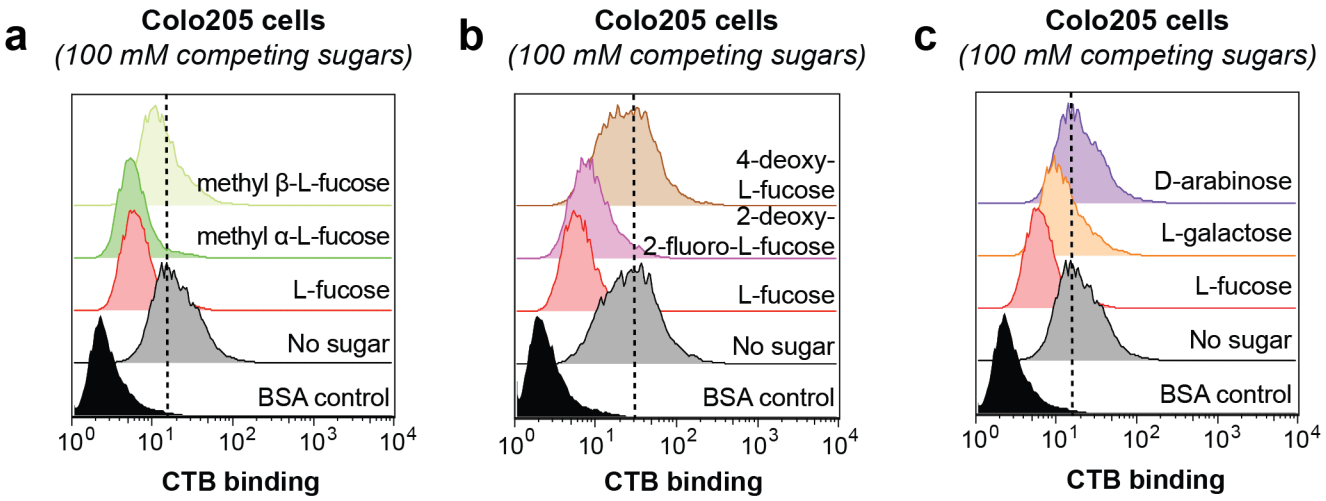

Figure S3. Flow cytometry histograms of CTB blocking by positional analogs of L-fucose. Inhibition of CTB binding to Colo205 cells was conducted with 100 mM competing sugars. Histograms are representative of a single trial from three independent experiments. (Data for position 1 analogs are shown in panel **a**, data for position 2 and 4 analogs are shown in panel **b**, and data for position 5 and 6 analogs are shown in panel **c**).

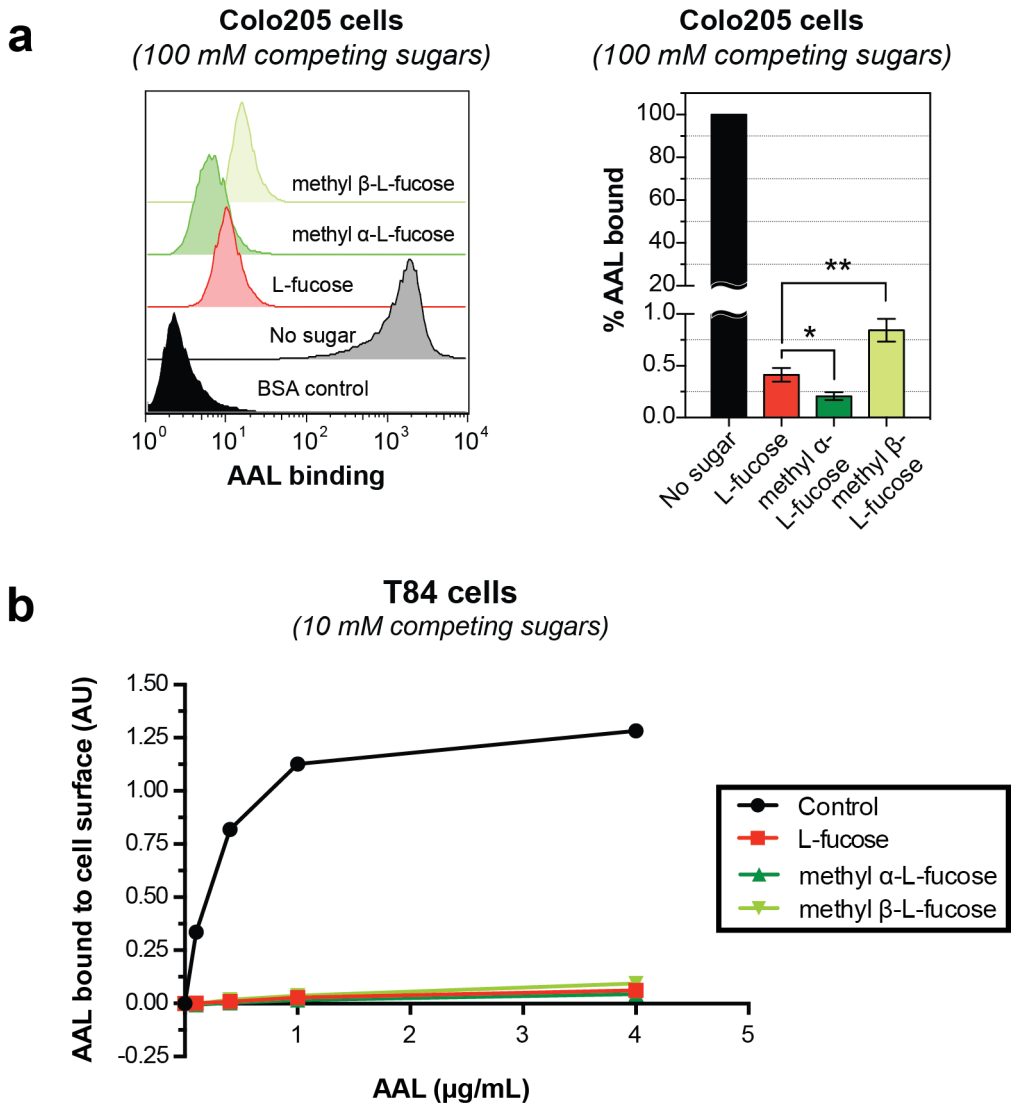

Figure S4. Blocking of AAL binding by position 1 analogs of L-fucose. (**a**) Inhibition of AAL binding to Colo205 cells with 100 mM competing sugars in a flow cytometry assay. Histograms are representative of a single trial from three independent experiments. Bar graph shown represents the average median fluorescence intensity (MFI) from three independent experiments and their standard deviations. Statistical significance determined by unpaired Welch's test: ** indicates a *p* value < 0.01 and * indicates a *p* value < 0.05. (**b**) Inhibition of AAL binding to T84 cells with 10 mM competing sugars as measured by ELISA. Error bars represent the standard deviation from the mean (n = 2).

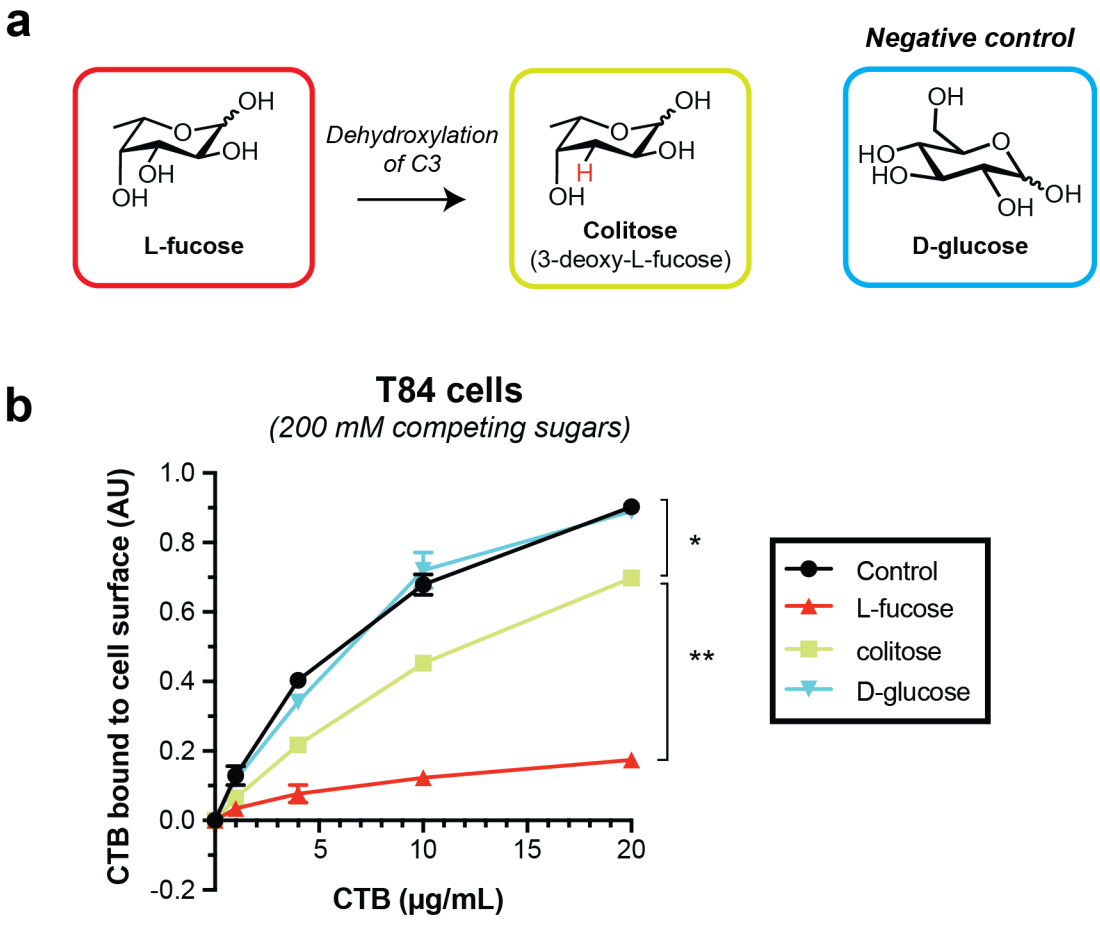

Figure S5. Blocking of CTB binding by L-colitose. (**a**) Monosaccharides used in this study. (**b**) Inhibition of CTB binding to T84 cells with 200 mM competing sugars as measured by ELISA. Error bars represent the standard deviation from the mean (n = 2). Statistical significance determined by unpaired Welch's test: ** indicates a *p* value < 0.01 and * indicates a *p* value < 0.05.

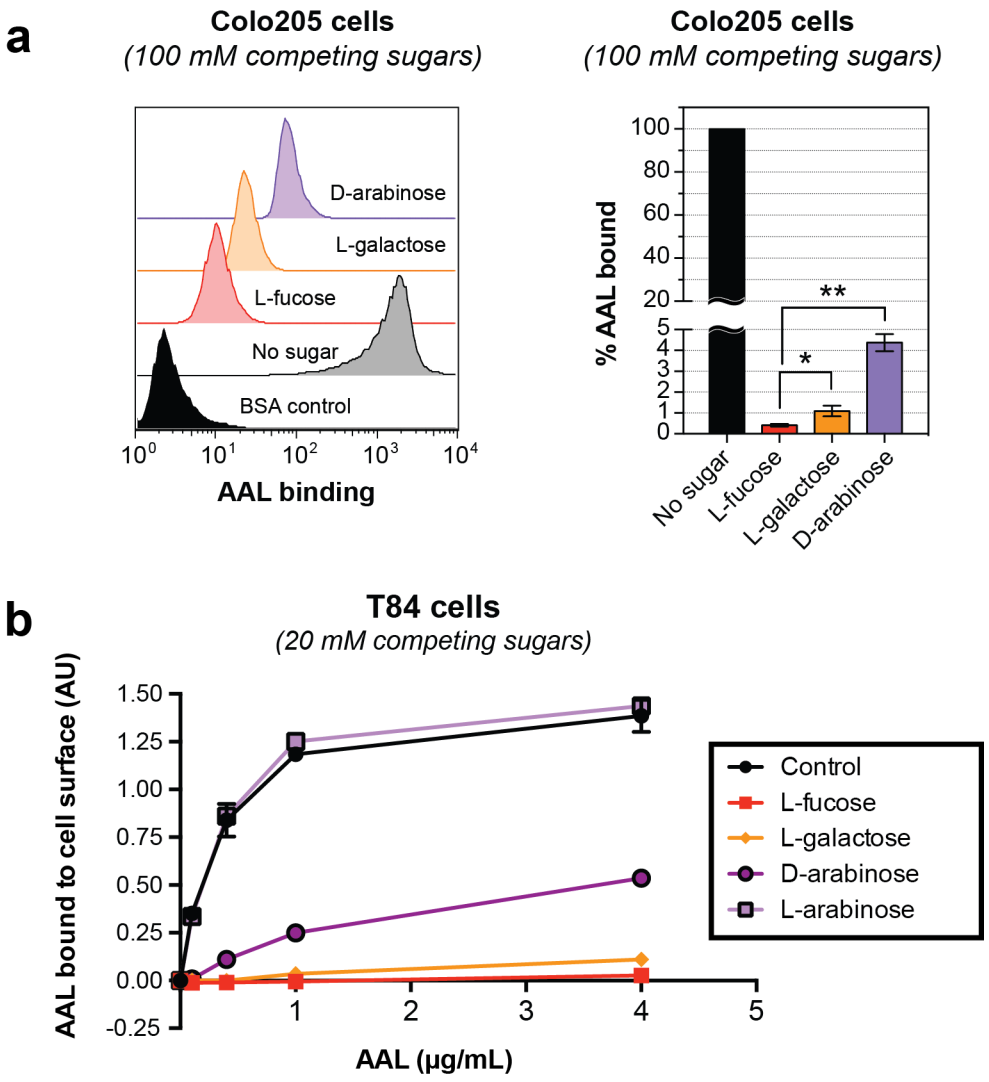

Figure S6. Blocking of AAL binding by position 5 and 6 analogs of L-fucose. (**a**) Inhibition of AAL binding to Colo205 cells with 100 mM competing sugars in a flow cytometry assay. Histograms are representative of a single trial from three independent experiments. Bar graph shown represents the average median fluorescence intensity (MFI) from three independent experiments and their standard deviations. Statistical significance determined by unpaired Welch's test: ** indicates a *p* value < 0.01 and * indicates a *p* value < 0.05. (**b**) Inhibition of AAL binding to T84 cells with 20 mM competing sugars as measured by ELISA. Error bars represent the standard deviation from the mean (n = 2).

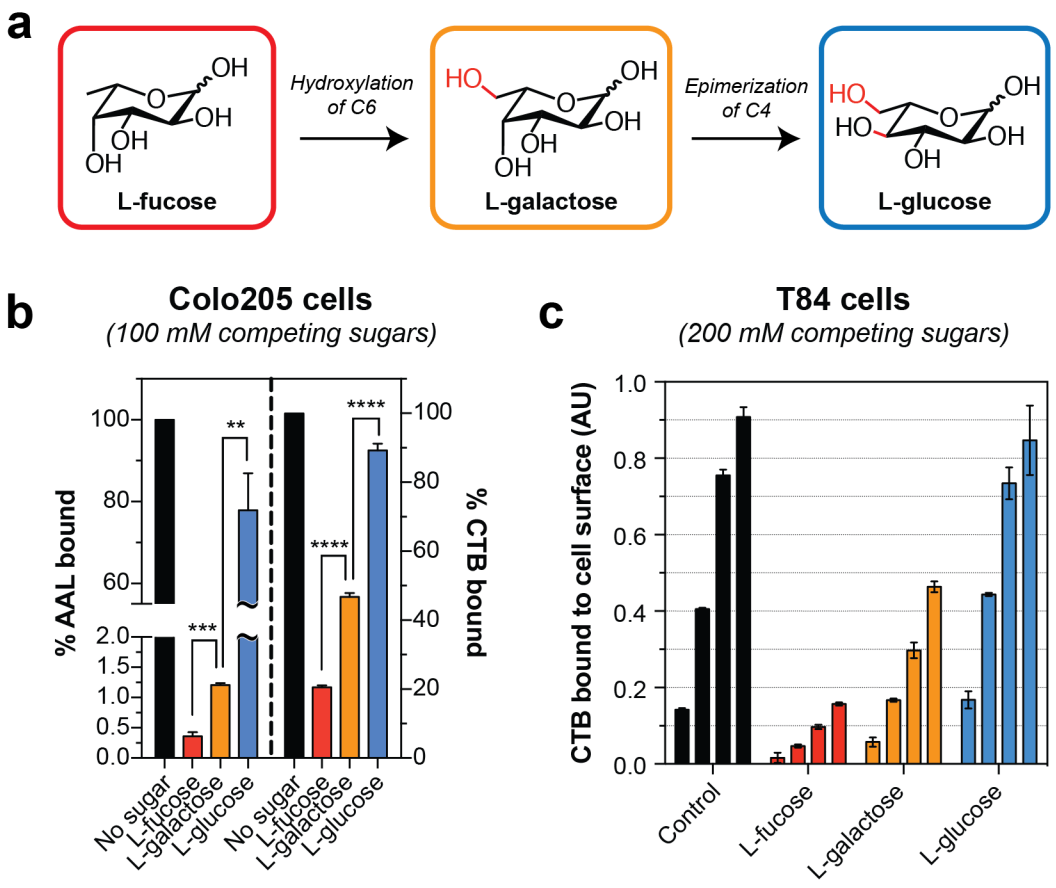

Figure S7. Blocking of CTB binding by L-glucose. (**a**) Monosaccharides used in this study. (**b**) Inhibition of AAL (*left*) and CTB (*right*) binding to Colo205 cells with 100 mM competing sugars in a flow cytometry assay. Bar graph shown represents the average median fluorescence intensity (MFI) from three independent experiments and their standard deviations. Statistical significance determined by unpaired Welch's test: **** indicates a *p* value < 0.0001, *** indicates a *p* value < 0.001, and ** indicates a *p* value < 0.01. (**c**) Inhibition of CTB binding to T84 cells with 200 mM competing sugars as measured by ELISA. Error bars represent the standard deviation from the mean (n = 2).

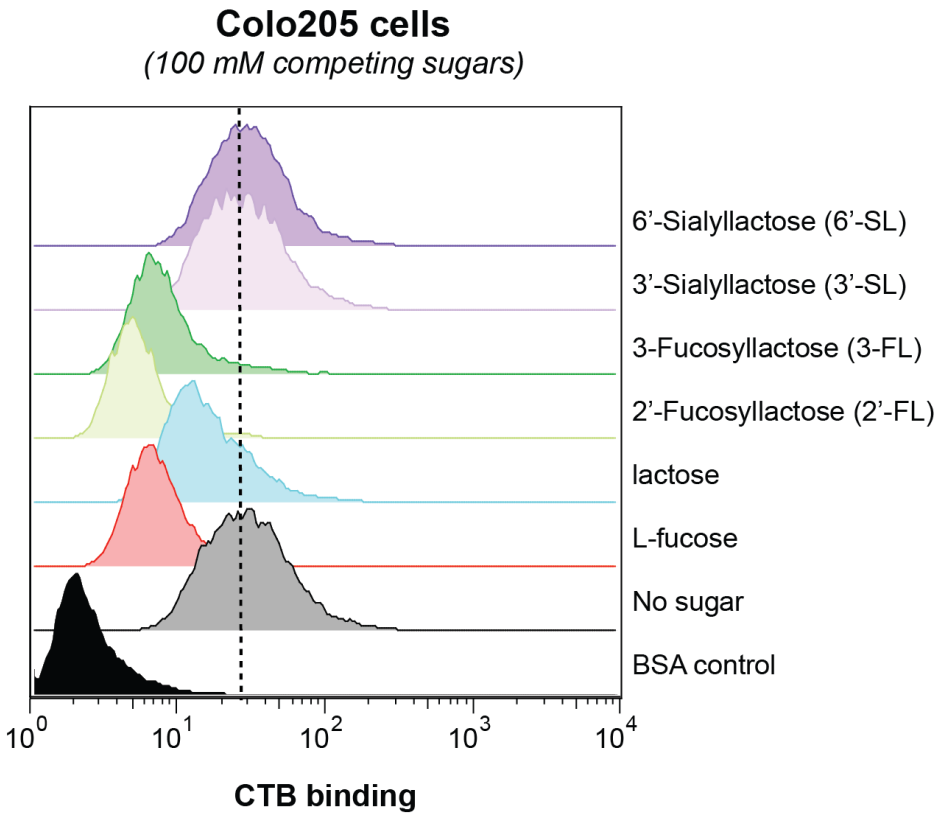

Figure S8. Flow cytometry histograms of CTB blocking by HMOs. Inhibition of CTB binding to Colo205 cells was conducted with 100 mM competing sugars. Histograms are representative of a single trial from three independent experiments.

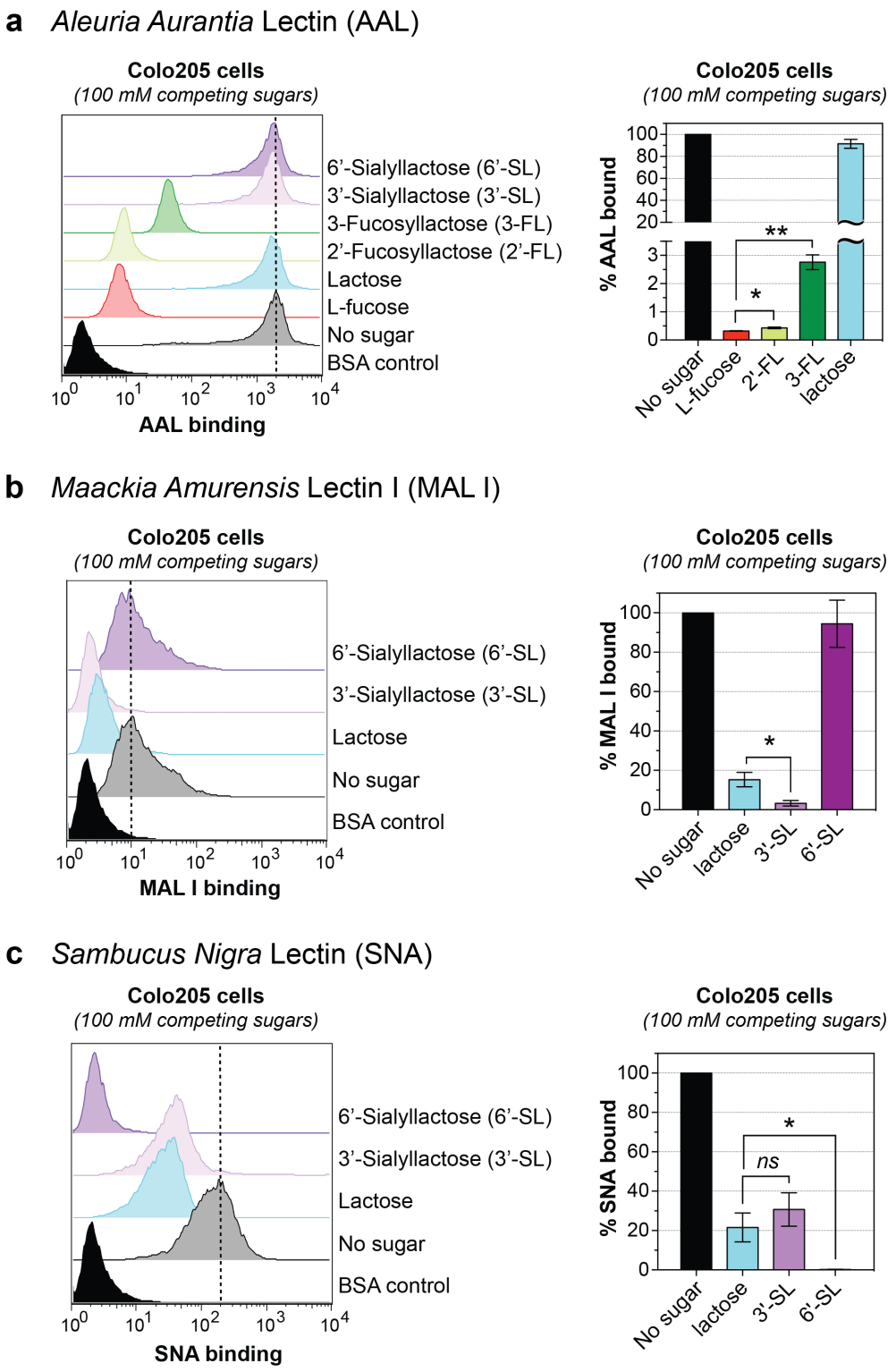

Figure S9. Blocking of lectin binding by HMOs. Inhibition of AAL (**a**), MAL I (**b**), and SNA (**c**) binding to Colo205 cells was conducted with 100 mM competing sugars. Histograms are representative of a single trial from three independent experiments. Bar graphs shown represent the average median fluorescence intensity (MFI) from three independent experiments and their standard deviations. Statistical significance determined by unpaired Welch's test: ** indicates a *p* value < 0.01 and * indicates a *p* value < 0.05. *ns* indicates difference not statistically significant.

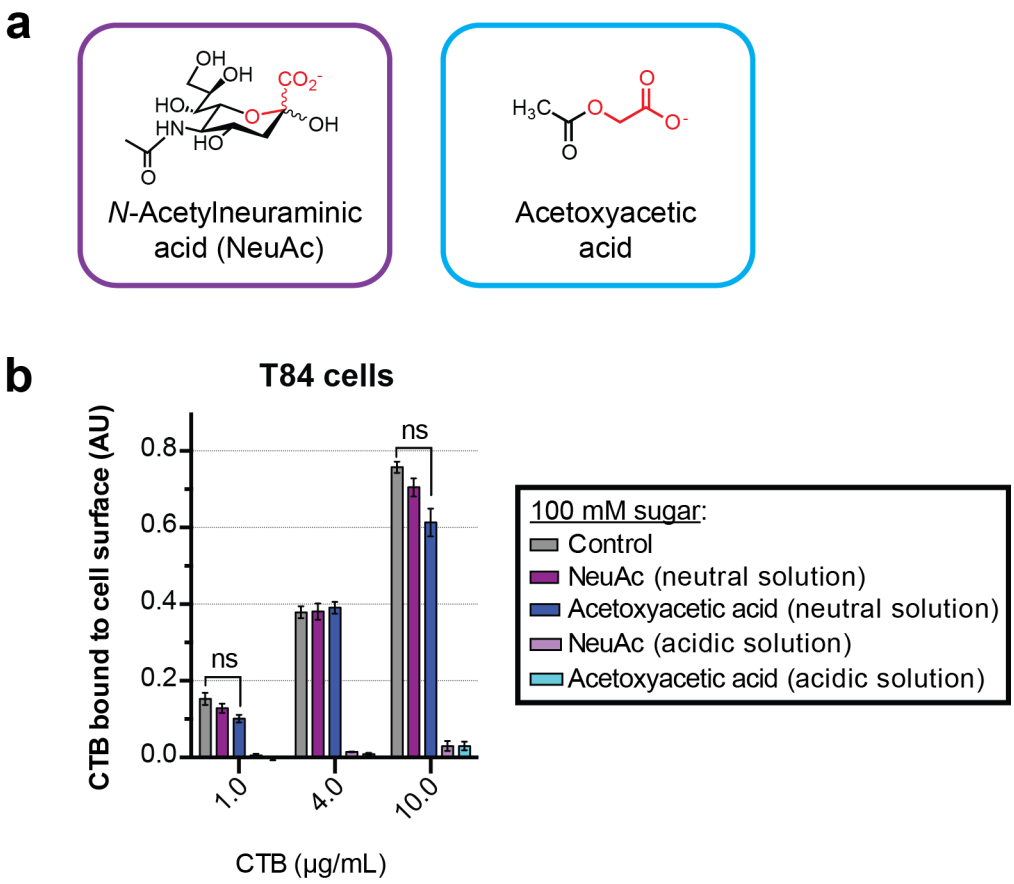

Figure S10. Acid washing of T84 cells with free *N*-acetylneuraminic acid (NeuAc). (**a**) *N*-acetylneuraminic acid or acetoxyacetic acid were either dissolved in binding buffer and left untreated (acidic solution of ~pH 3) or neutralized with equimolar sodium bicarbonate (neutral solution of ~pH 6-7). (**b**) Inhibition of CTB binding to T84 cells with 100 mM competing sugars as measured by ELISA. Error bars represent the standard deviation from the mean (n = 2). Statistical significance determined by unpaired Welch's test: *ns* indicates difference not statistically significant.

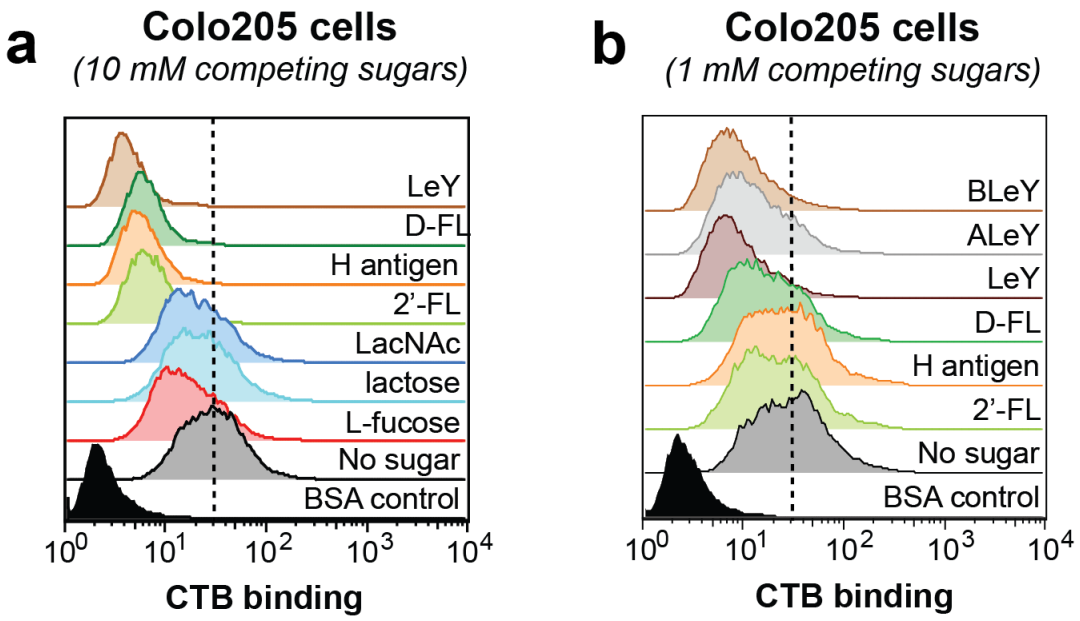

Figure S11. Flow cytometry histograms of CTB blocking by stepwise conversion of 2'-FL to A/BLeY. (**a**) Inhibition of CTB binding to Colo205 cells was conducted with 10 mM of 2'-FL, H antigen, DF-L, or LeY. Histograms are representative of a single trial from three independent experiments. (**b**) Inhibition of CTB binding to Colo205 cells was conducted with 1 mM of LeY, ALeY, or BLeY. Histograms are representative of a single trial from three independent experiments.

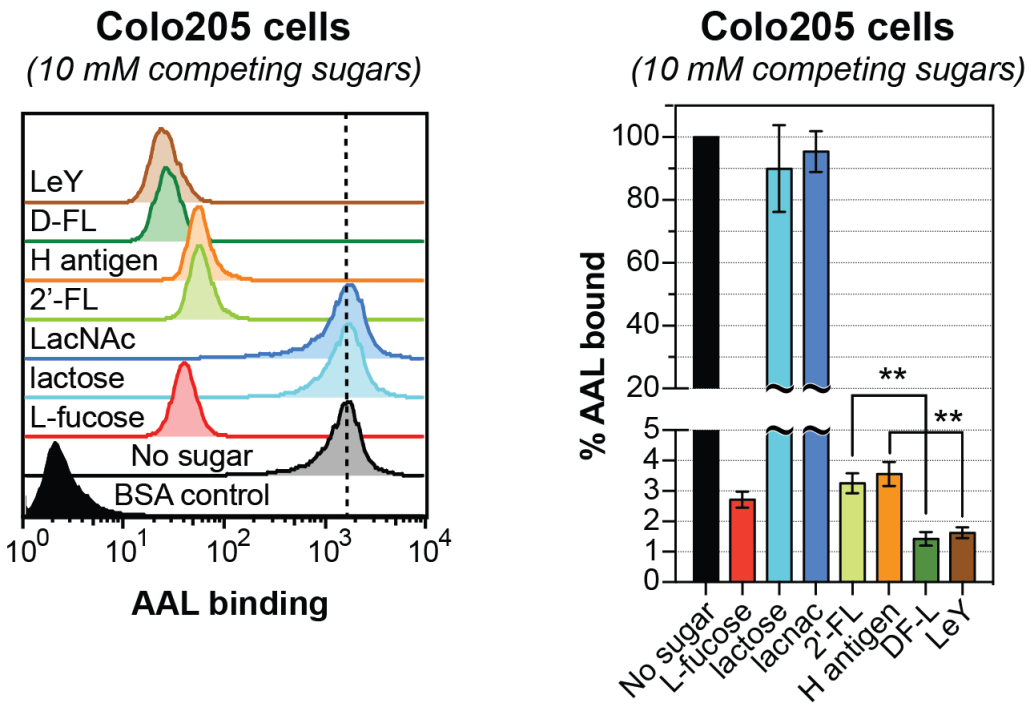

Figure S12. Blocking of AAL binding by 2'-FL, H antigen, DF-L, and LeY. Inhibition of AAL binding to Colo205 cells with 10 mM competing sugars in a flow cytometry assay. Histograms are representative of a single trial from three independent experiments. Bar graph shown represents the average median fluorescence intensity (MFI) from three independent experiments and their standard deviations. Statistical significance determined by unpaired Welch's test: ** indicates a *p* value < 0.01.

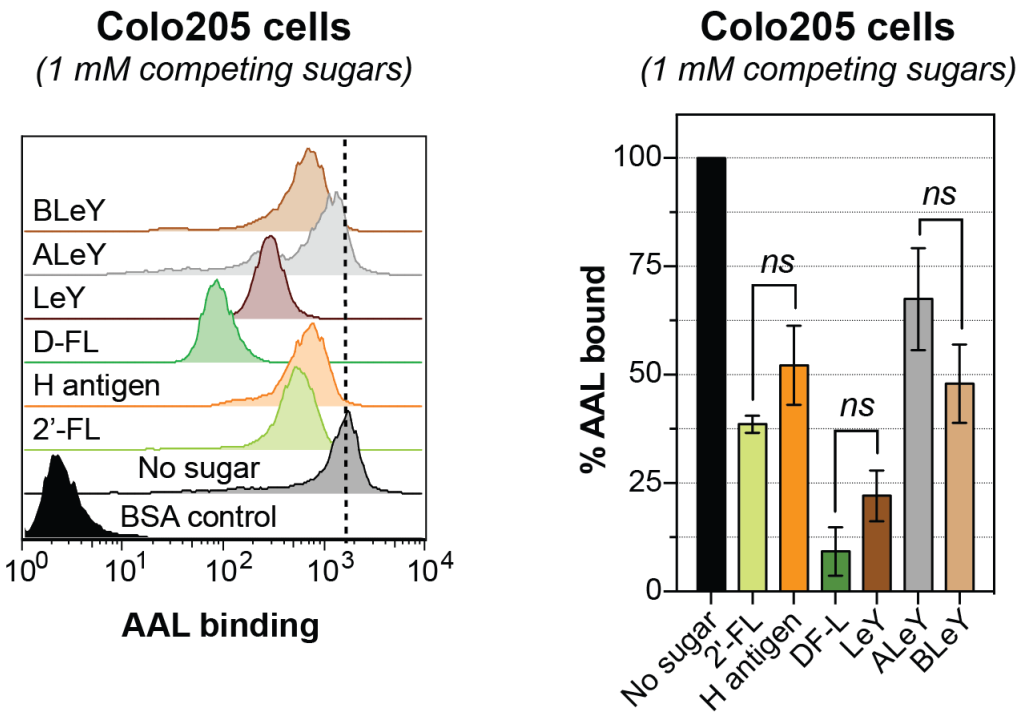

Figure S13. Blocking of AAL binding by LeY, ALeY, and BLeY. Inhibition of AAL binding to Colo205 cells with 1 mM competing sugars in a flow cytometry assay. Histograms are representative of a single trial from three independent experiments. Bar graph shown represents the average median fluorescence intensity (MFI) from three independent experiments and their standard deviations. Statistical significance determined by unpaired Welch's test: *ns* indicates difference not statistically significant.

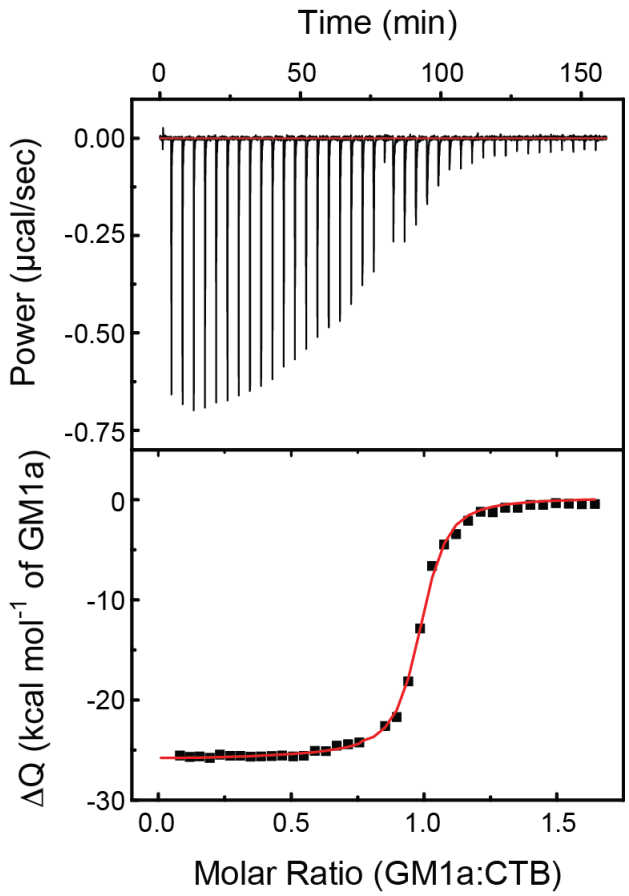

Figure S14. ITC measurement of 100 µM GM1a titrated to 30 µM CTB in PBS pH 7.4. Top panel represents the power recorded during titration and bottom panel the integrated heats per mol GM1a obtained by integration of the peaks and subtraction of the dilution of GM1a into buffer. The red line shows the one-site fitting (see Table S3).

Table S3. Parameters obtained from fitting of the ITC data with a one-site model.

	GM1a	LeY
n	0.970 ± 0.002	1[a]
Kd	58 nM +/- 5 nM	1.4 mM +/- 0.05 mM
dH (cal/mol)	-2.58E4 ± 100	-7240 ± 730
dS (cal/mol/deg)	-53.4	-11.2

[a]n was set to 1 for LeY.

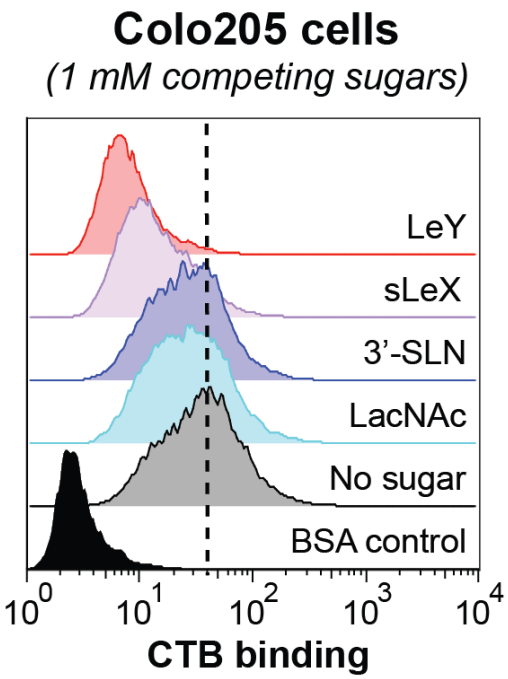

Figure S15. Flow cytometry histograms of CTB blocking by 3'-SLN, sLeX, and LeY. Inhibition of CTB binding to Colo205 cells was conducted with 1 mM competing sugars. Histograms are representative of a single trial from three independent experiments.

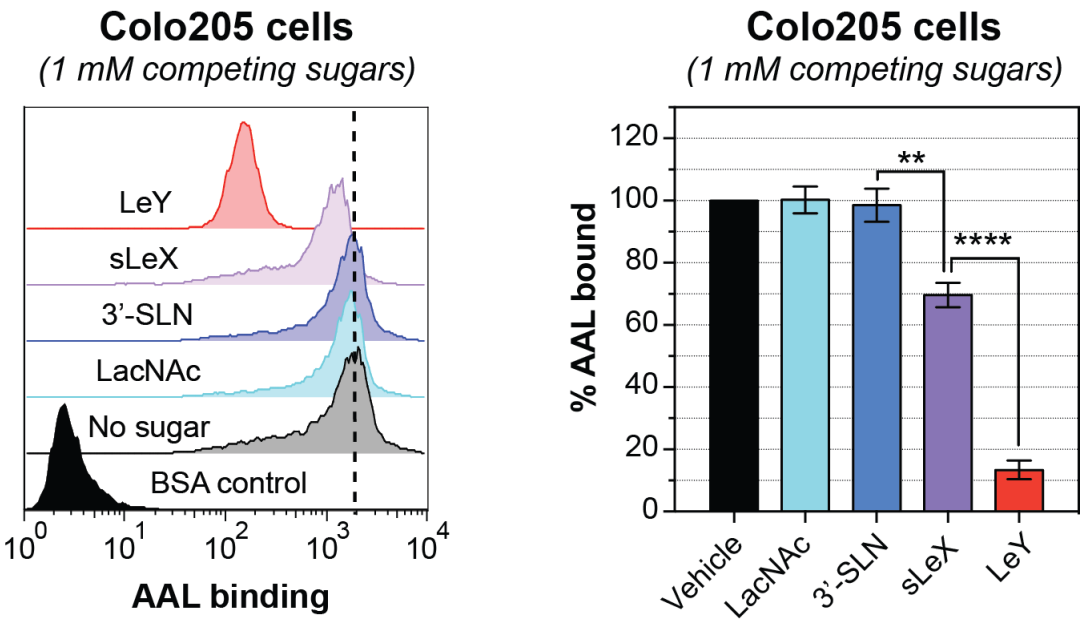

Figure S16. Blocking of AAL binding by 3'-SLN, sLeX, and LeY. Inhibition of AAL binding to Colo205 cells with 1 mM competing sugars in a flow cytometry assay. Histograms are representative of a single trial from three independent experiments. Bar graph shown represents the average median fluorescence intensity (MFI) from three independent experiments and their standard deviations. Statistical significance determined by unpaired Welch's test: **** indicates a *p* value < 0.0001 and ** indicates a *p* value < 0.01.

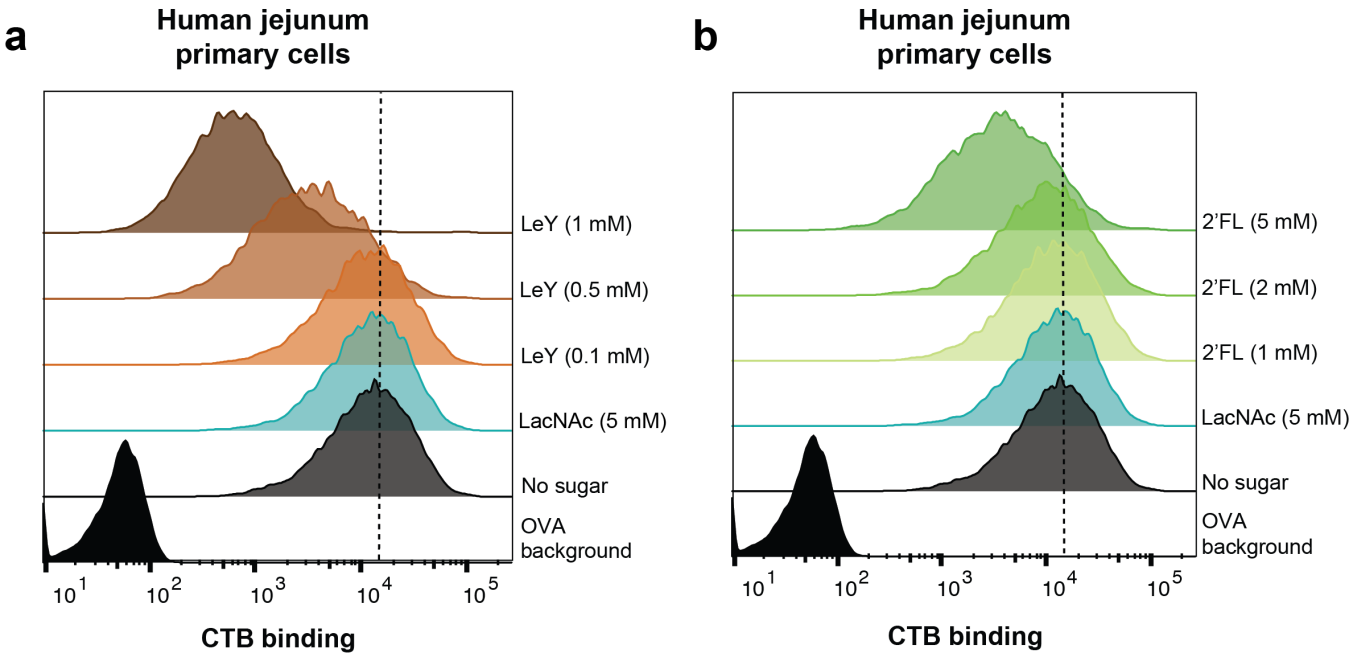

Figure S17. Flow cytometry histograms of CTB blocking by LeY, 2'-FL, and LacNAc to human jejunum primary cells. A representative histogram on CTB binding to freshly isolated human jejunal epithelial cells (EpCAM+, CD45 negative), from one patient, after pre-incubation of CTB with LeY (panel **a**), 2'-FL (panel **b**), or LacNAc (both panels **a** and **b**) at various concentrations. OVA staining used as a background control.

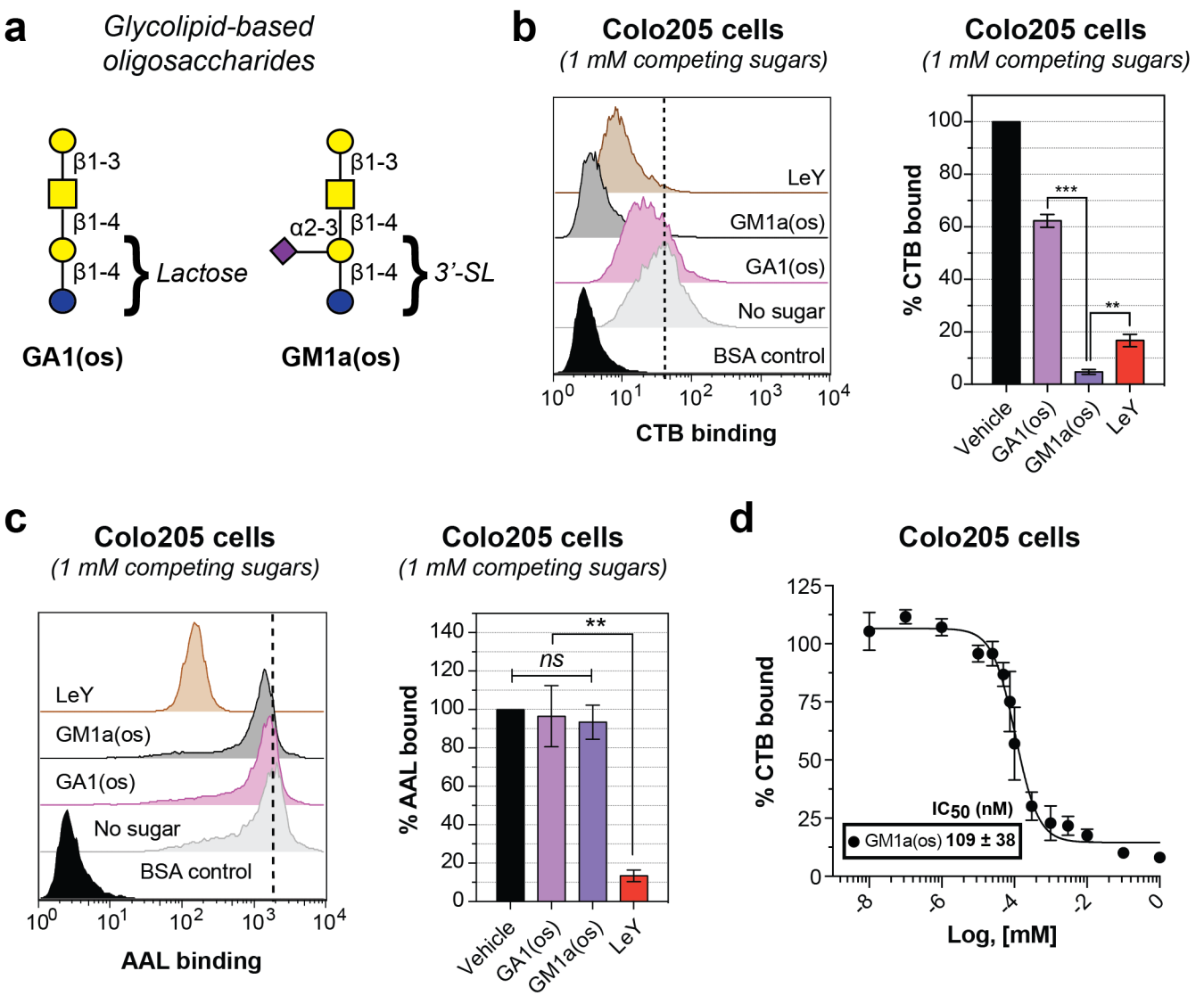

Figure S18. Blocking of CTB and AAL binding to Colo205 cells by GA1(os), GM1a(os), and LeY. (**a**) Glycolipid-derived oligosaccharides used in this study. Inhibition of CTB (**b**) and AAL (**c**) binding to Colo205 cells with 1 mM competing sugars in a flow cytometry assay. Histograms are representative of a single trial from three independent experiments. Bar graphs shown represent the average median fluorescence intensity (MFI) from three independent experiments and their standard deviations. Statistical significance determined by unpaired Welch's test: *** indicates a *p* value < 0.001, ** indicates a *p* value < 0.01, and *ns* indicates difference not statistically significant. (**d**) Dose-dependent inhibition of CTB binding to Colo205 cells in a flow cytometry assay. Error bars represent the standard deviation from the mean (n = 3). IC_{50} values were calculated for individual replicates using GraphPad Prism software and then averaged.

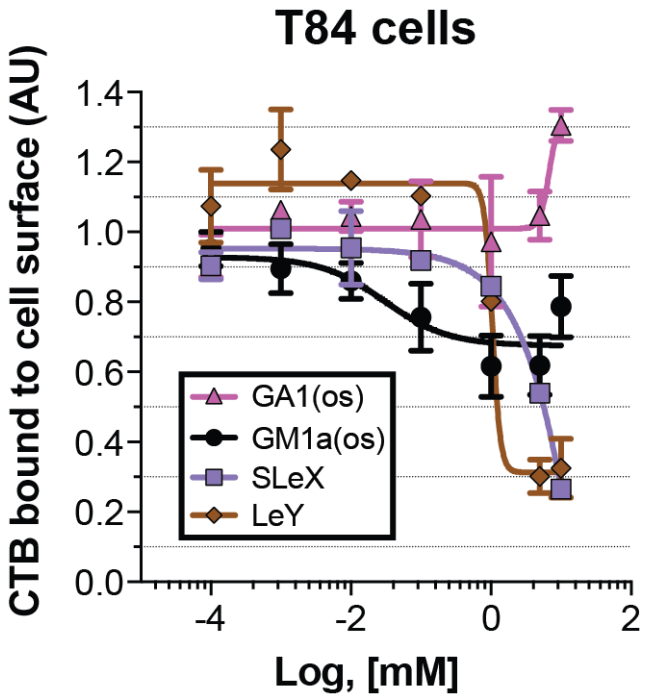

Figure S19. Blocking of CTB binding to T84 cells by GA1(os), GM1a(os), sLeX, and LeY. Dose-dependent inhibition of CTB binding to T84 cells measured by ELISA. Error bars represent the standard deviation from the mean (n = 2).

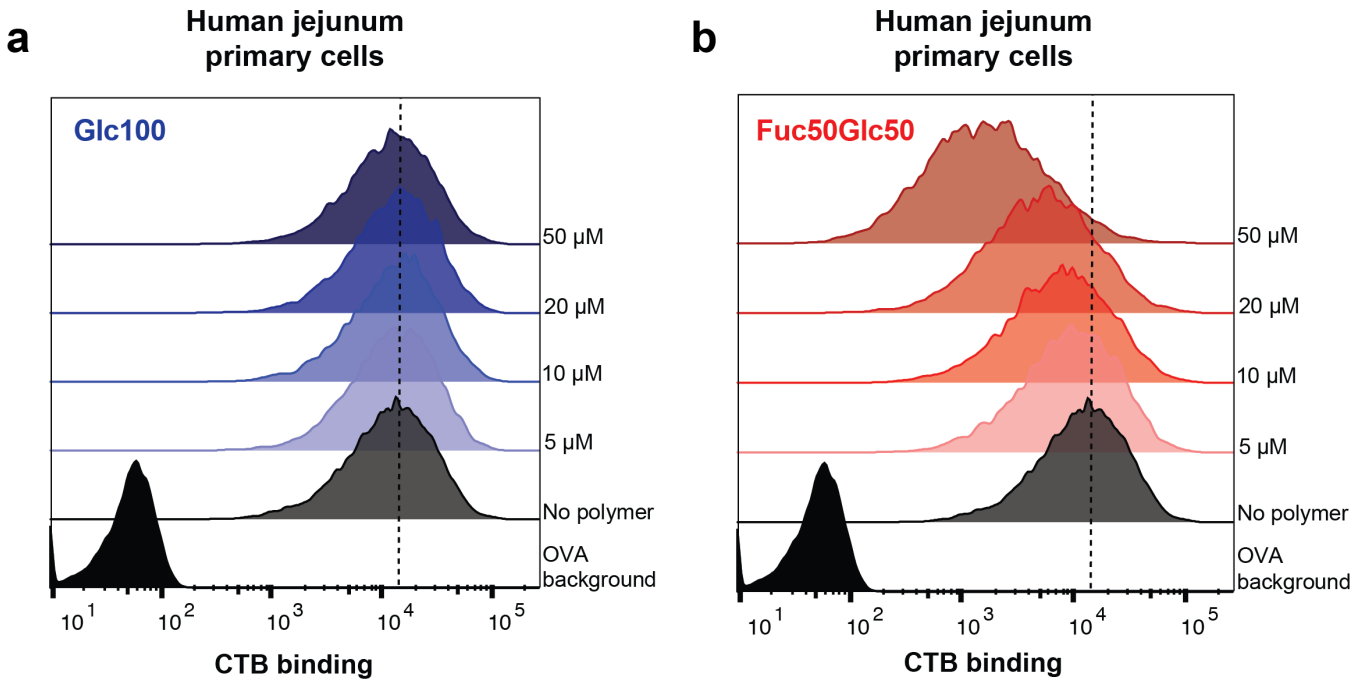

Figure S20. Flow cytometry histograms of CTB blocking by Glc100 and Fuc50Glc50 polymers to human jejunum primary cells. A representative histogram of CTB binding to freshly isolated human jejunal epithelial cells (EpCAM+, CD45 negative), from one patient, after pre-incubation of CTB with Glc100 polymer (panel **a**) or Fuc50Glc50 polymer (panel **b**) at various concentrations. OVA staining used as a background control.

References:

1. Lloyd, D. and Bennett, C. S. (2014) Gram-scale synthesis of an armed colitose thioglycoside, *J. Org. Chem.* 79, 9826-9829 DOI: 10.1021/jo501472v
2. Lindhorst, T. K., and Thiem, J. (1990) The synthesis of 3-deoxy-L-fucose (3,6-dideoxy-L-xylo-hexose), *Liebigs Annalen der Chemie* 1990, 1237-1241 DOI: 10.1002/jlac.1990199001222
3. Love, J. A., Morgan, J. P., Trnka, T. M., and Grubbs, R. H. (2002) A practical and highly active ruthenium-based catalyst that effects the cross metathesis of acrylonitrile, *Angew. Chem. Int. Ed. Engl.* 41, 4035-4037 DOI: 10.1002/1521-3757(20021104)114:21<4207::AID-ANGE4207>3.0.CO;2-G
4. Wu, L., and Sampson, N. S. (2014) Fucose, mannose, and beta-N-acetylglucosamine glycopolymers initiate the mouse sperm acrosome reaction through convergent signaling pathways, *ACS Chem. Biol.* 9, 468-475 DOI: 10.1021/cb400550j